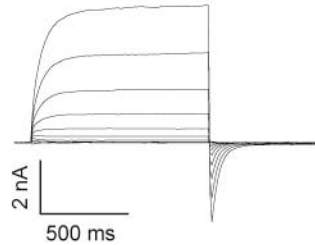


Supplemental information 1

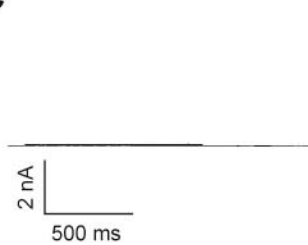
A

	exon 21
NP_848757	YMEMIIQFGFVTLFVASFPLAPLFALLNNIIIEIRLDAAKKFVTELRRPVAIRAKDIGIWN 819
NP_705817	YMEMIIQFGFVTLFVASFPLAPVFALLNNNIEIRLDAAKFVTELRRPAVRTKDIGIWF 803
NP_996914	YLEMVLQFGFVTTIFVAACPLAPLFALLNNNVEIRLDARKFCEYRRPVAERAQDIGIW 704
NP_001121575	YLEMVLQFGFTTIFVAAFPLAPLALLNNIIIEIRLDAYKFTQWRRPLPARATDIGIWL 814
NP_848888	YLEMILQFGFATLFVASFPLAPLFALMNNIMGRVDWKLTIQYRRPVAAKHSIGVWQD 601
NP_808362	YLEMIIQFGFVTLFVASFPLAPLALLVNNEIRVDWKLTIQFRRMVPEKAQDIGAWQP 748
NP_001240742	FMEMMIQYGFETIFVAAFPLAPLALFSNLVEIRLDAAIKMVRQLQRRLVPRKAKDIGTWLQ 591
NP_848468	YQEMFVQFGYVVLFSSAFPLAALCALVNNLIEIRSDAFKLCTGLQRPFGRRVESIGQWQK 802
NP_001158151	YLELFLQFGYVSLFSCVYPLAAAFAVLNNFTEVNSDALKMCRVFKRPFAEPSASIGVWQL 557
NP_598740	

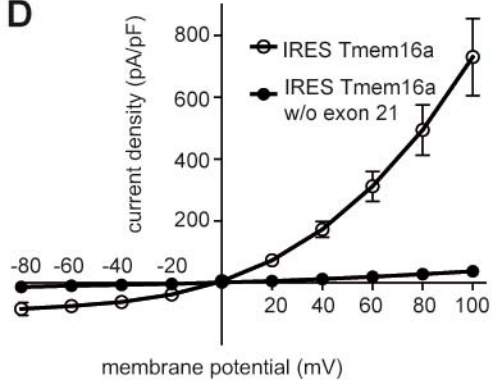
B



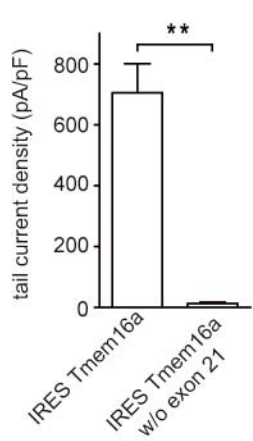
C



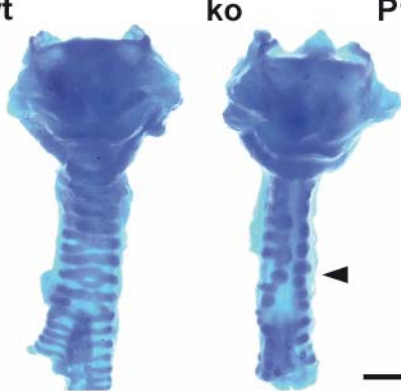
D



E



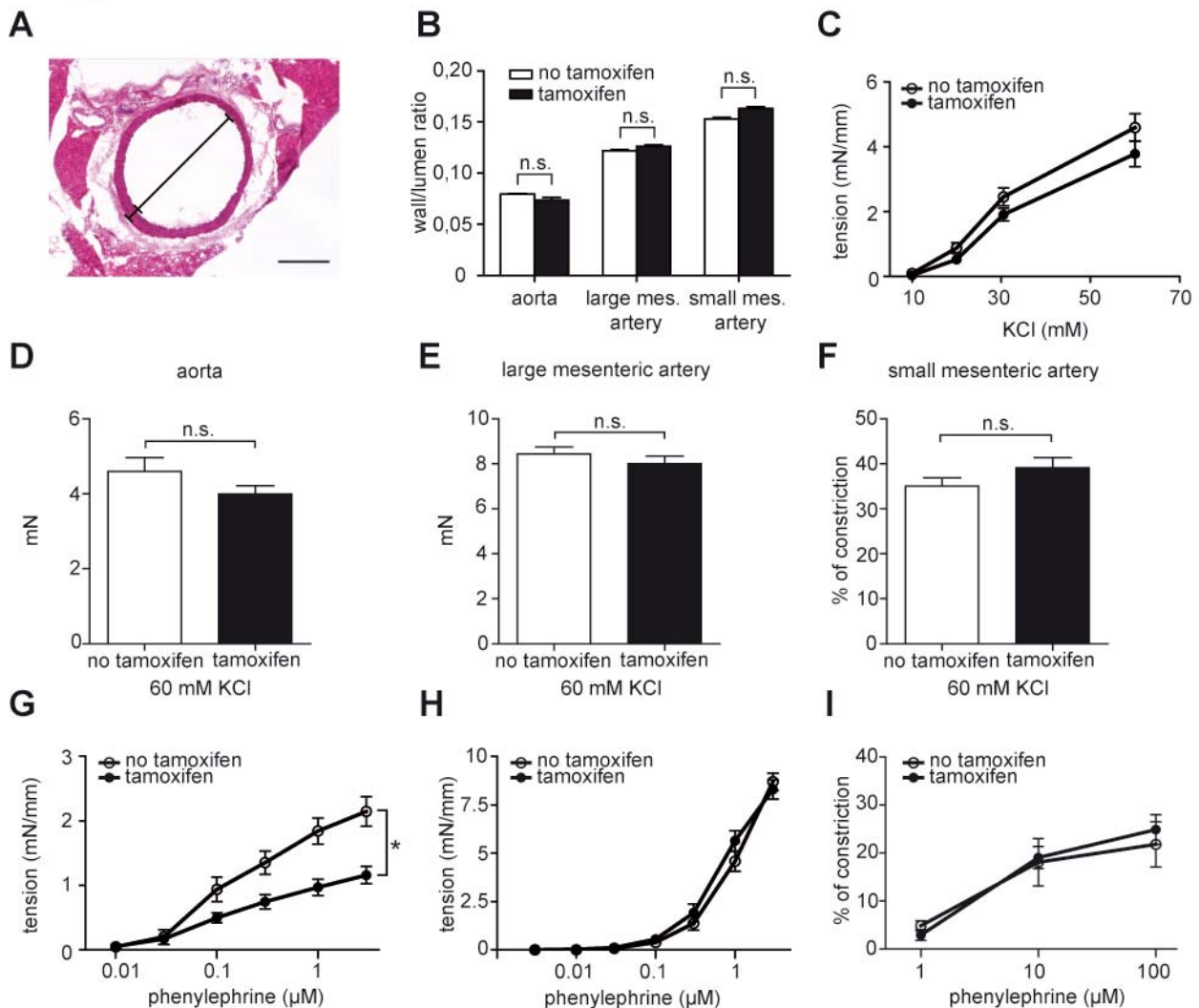
F



Supplemental information 1

(A) Alignment for the amino acid sequence encoded by *Tmem16a* exon 21 with the family of TMEM16 proteins generated with Clustal alignment program (55). (B,C) Typical patch-clamp recordings of HEK293 cells transfected with either a cDNA encoding wild-type TMEM16A (B) or a variant devoid of exon 21 (C). Cells were clamped to voltages between -80 mV and +100 mV in 20 mV steps, followed by a voltage jump to -80 mV. (D) Current densities for TMEM16A and TMEM16A without exon 21 measured in transfected HEK293 cells 1 s after depolarization steps to the indicated voltage as described for (B). (E) Tail current densities for TMEM16A wild-type and TMEM16A without exon 21 in transfected HEK293 cells ($n = 12$ in each group). (F) In contrast to wild-type, the cervical situs of a 2-days-old knockout mouse (right) revealed abnormal tracheal cartilages (arrowhead).

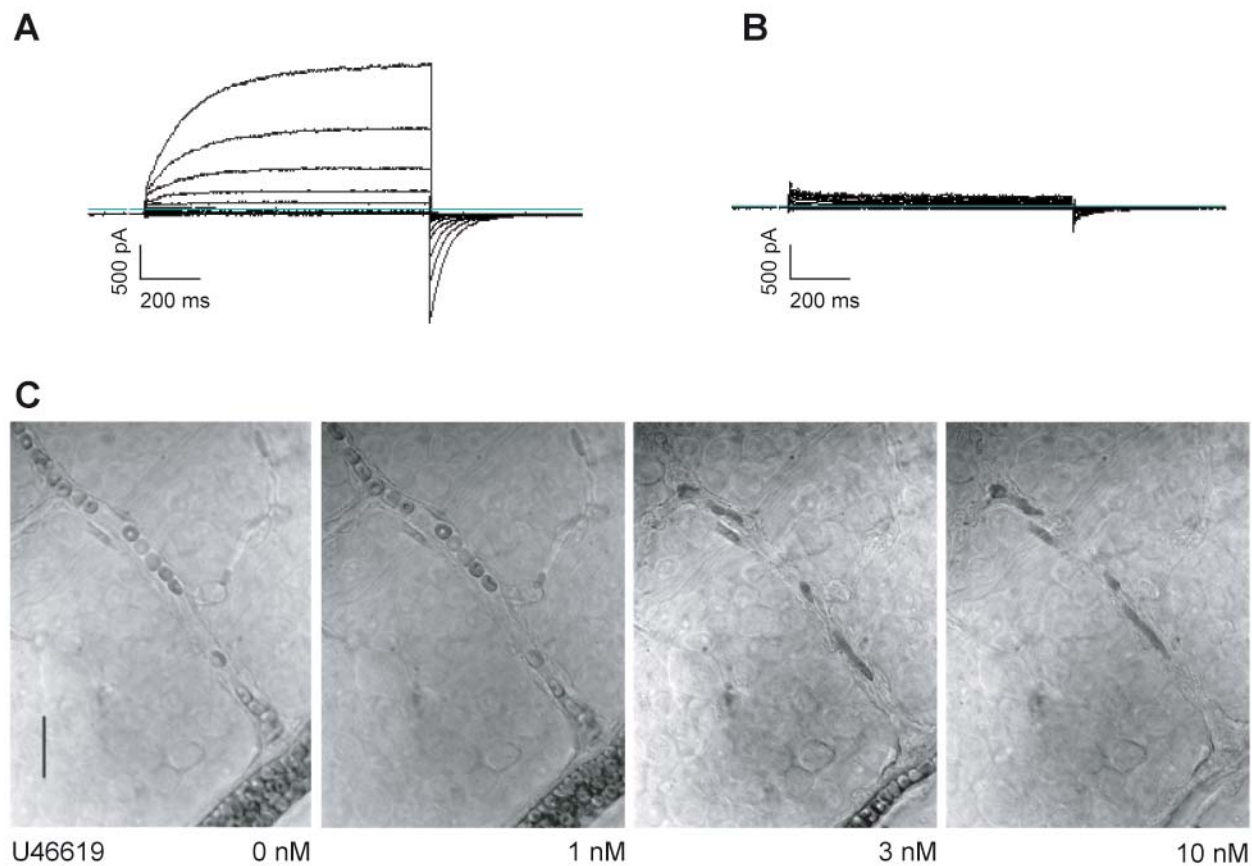
Supplemental information 2



Supplemental information 2

(**A,B**) Wall-to-lumen ratio determined in transversal sections of HE stained blood vessels ($n = 3$ mice per group). Scale bar 500 μ m. n.s.: not significant; Student's t-test; $p > 0.05$. (**C**) Contractile effects of different extracellular KCl concentrations on aortic rings. (**D,E**) Contractile effects of 60 mM KCl on aortic (**D**) and 1st/2nd order mesenteric artery rings (**E**) determined by wire myography. (**F**) Changes in diameter of pressurized 3rd/4th order mesenteric arteries at 60 mM KCl determined by videomicroscopy. (**G,H**) Dose-response curves for the contractile effects of phenylephrine for aortic rings (**G**; $n = 6$ in each group) and for 1st and 2nd order mesenteric artery rings (**H**; $n = 16$ to 24 in each group) determined by wire myography. 2-way-ANOVA; *: $p < 0.05$; **: $p < 0.01$. (**I**) Change in diameter of pressurized 3rd and 4th order mesenteric arteries by phenylephrine determined by videomicroscopy ($n = 4$ to 6 in each group).

Supplemental information 3



Supplemental information 3

(**A,B**) Typical currents recorded from pericytes isolated from brain of non-induced control mice (**A**) and induced conditional TMEM16A knockout mice (**B**). (**C**) Representative time lapse images showing a constriction of a primary and higher order retinal arteriole of non-induced control mice taken 20 min after application of the indicated concentration of the vasoconstrictor U46619. Scale bar: 20 μ m.